Microscopic description of protein thermostabilization mechanisms with disaccharides from Raman spectroscopy investigations

2007 J. Phys.: Condens. Matter 19 205142

(http://iopscience.iop.org/0953-8984/19/20/205142)

IOP Publishing Journal of Physics: Condensed Matter

J. Phys.: Condens. Matter **19** (2007) 205142 (8pp) doi:10.1088/0953-8984/19/20/205142

Microscopic description of protein thermostabilization mechanisms with disaccharides from Raman spectroscopy investigations

A Hédoux, F Affouard, M Descamps, Y Guinet and L Paccou

Laboratoire de Dynamique et Structure des Matériaux Moléculaires UMR CNRS 8024, Université de Lille 1, UFR de Physique, Bâtiment P5, 59 655 Villeneuve d'Ascq Cedex, France

Received 3 January 2007
Published 25 April 2007
Online at stacks.iop.org/JPhysCM/19/205142

Abstract

The mechanisms of protein thermostabilization by sugar were analysed for three disaccharides (maltose, sucrose and trehalose) characterized by the same chemical formula ($C_{12}H_{22}O_{11}$). Raman scattering investigations simultaneously carried out in the low-frequency range and in the amide I band region provide a microscopic description of the process of protein thermal denaturation. From this detailed description, the influence of sugar on this process was analysed. The principal effect of sugars is to stabilize the tertiary structure, in which the biomolecule preserves its native conformation, through a strengthening of O–H interactions. This study shows that the bioprotective properties of sugars are mainly based on interactions between water and sugar. The exceptional properties of trehalose to preserve the native state of lysozyme by heating can be associated with its capability to distort the tetra-bonded hydrogen bond network of water.

(Some figures in this article are in colour only in the electronic version)

1. Introduction

Proteins are the principal units that govern the functions of living systems. Under extreme conditions (temperature, high pressure, desiccation) proteins may denature. Trehalose is recognized to be very effective in the stabilization of macromolecules against thermal inactivation [1] and of labile proteins during freeze-drying [2] and exposure to high temperatures in solutions [3]. Several hypotheses have been suggested to explain the superior effectiveness of trehalose with regard to other sugars. Some of them involve (i) direct biomolecule–sugar–water interactions [3, 4], (ii) specific properties of sugar–water solutions concerning the vitrification of the solutions [5] and (iii) the 'destructuring effect' of sugars on the water tetrahedral H-bond network [6]. Extended investigations of water–sugar solutions have revealed specific signatures of trehalose with respect to other sugars both in the physical

0953-8984/07/205142+08$30.00

properties (fragility) of the solutions [5, 7–9] (fragility, T_g value) and the destructuring effect of the water H-bond network [10–13]. However, investigations on protein–water–sugar systems are much more sparse [14, 15].

Previous Raman scattering investigations simultaneously carried out in the low-frequency range (10 cm^{-1}, 300 cm^{-1}) and in the amide I band region (1500 cm^{-1}, 1800 cm^{-1}) have given a microscopic description of protein thermal denaturation [16] as a two-stage process. The first stage corresponds to a transformation of the tertiary structure into a more flexible configuration, without unfolding of the secondary structure, accompanied by solvent penetration inside the protein. This transformation appears as a precursor of the second stage, i.e. the unfolding process. Moreover, dissolving lysozyme in D_2O is very useful to analyse water–protein interactions through H/D exchange, easily detected by Raman spectroscopy.

This paper focuses on the protective action of additive sugars in lysozyme–water solution during the process of thermal denaturation. The analysis of three disaccharides characterized by the same chemical formula ($C_{12}H_{22}O_{11}$) and the same number of hydroxyl groups can be used to determine the specific properties of trehalose which make it a better bioprotector than other disaccharides.

2. Material and methods

Lysozyme from chicken egg white (14.3 kDa) is supplied from Sigma. High purity maltose monohydrate, sucrose and trehalose dihydrate were supplied from Fluka and Sigma. First the sugar–water mixtures were prepared at the appropriate concentration, and thereafter the protein was added. Ternary solutions with 40% mass sugar concentration dissolved in H_2O (W_hLM40, W_hLS40, W_hLT40) and in D_2O (W_dLM40, W_dLS40, W_dLT40) were systematically analysed by Raman scattering. The protein containing mixtures were agitated in an Eppendorf agitator at about 298 K with about 1000 turn/min. Sugar/water weight proportions were prepared using double distilled pure water. The lysozyme concentration of about 14.58×10^{-3} M l^{-1} was used to ensure about 10 water hydration shells surrounding the protein molecules in water that limits the direct protein–protein interactions. Measurements were carried out in the 295–380 K temperature range on samples at pH 6.5.

Raman spectra were recorded in the 10–300 cm^{-1}, 1500–1800 cm^{-1} spectral windows. The spectra were measured in back-scattering geometry, using an XY Dilor spectrometer with a 514.5 nm Ar–Kr laser and 20 mW power incident line. The mixtures were loaded in hermetically closed Hellma quartz Suprasil cells.

3. Results

3.1. In the low-frequency range

The scattered low-frequency intensity is composed of quasielastic intensity and harmonic vibrations which overlap in the 10–100 cm^{-1} range. An appropriate treatment of the low-frequency data, detailed in a previous work [16], gives the Raman susceptibility ($\chi''(\nu)$) related to the vibrational density of states ($g(\nu)$, VDOS) by $\chi''(\nu) = \frac{C(\nu)g(\nu)}{\nu}$, where $C(\nu)$ is the light–vibration coupling coefficient. It is usually observed that $C(\nu)$ has a linear ν-dependence in the boson peak (BP) region [17–19], and the Raman susceptibility is then considered as representative of the VDOS ($\chi''(\nu) \propto g(\nu)$). The Raman susceptibilities of dry lysozyme (DL) and water–lysozyme mixture (WL) at room temperature and at 345 K are plotted in figure 1. At room temperature, the spectrum is composed of two broad bands. From a previous study [16], the low-frequency band was considered as reflecting principally the VDOS of

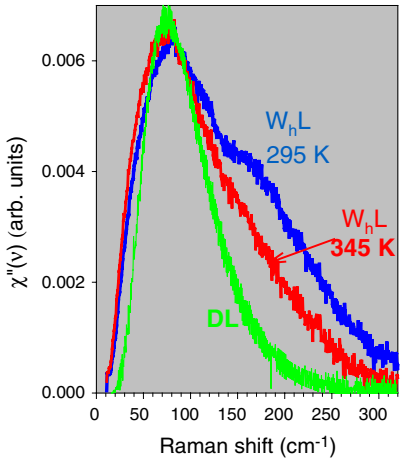

Figure 1. Raman susceptibility in dry lysozyme (DL) at room temperature and hydrated lysozyme (W_hL) at room temperature and at 345 K.

lysozyme while the high-frequency band was assigned to the intermolecular O–H stretching vibrations in bulk water. An excess of VDOS with respect to the dry lysozyme can be observed in the very low-frequency range. This excess of VDOS is assigned to the dynamics of the water–protein interface, probably corresponding to confined water inside protein, in accordance with previous inelastic neutron scattering studies [20, 21]. On heating, the Raman susceptibility undergoes significant transformations, shown at 345 K in figure 1. Above 345 K no additional transformation of the Raman susceptibility is observed, and then it remains similar in the denatured state. At 345 K, the high-frequency band is almost not observed, indicating the breaking of the H-bond network in water. As a consequence, the tertiary structure of the protein becomes highly flexible [16], inducing the solvent penetration inside the protein, associated with the enhancement of the excess of VDOS in the low-frequency range at 345 K.

3.1.1. Influence of sugars on the low-frequency Raman spectrum of hydrated lysozyme in the native and denatured states. In the native state ($T = 303$ K) each spectrum is composed of two broad bands as for hydrated lysozyme (W_hL). Only the Raman susceptibility of the W_hLT40 sample is compared to that of W_hL in figure 2 for better clarity, the spectrum of each ternary mixture being very similar. Addition of sugar in hydrated lysozyme induces two main changes in the Raman susceptibility indicated by arrows in figure 2(a). The first arrow shows an enhancement of the VDOS in the very low-frequency range, corresponding to increased solvent–lysozyme interactions in the solvent–protein interface in ternary mixtures with regard to hydrated lysozyme, probably via hydrogen bonds. The second arrow shows the decrease of the susceptibility of the broad band with addition of sugar, indicative of the distortion of the tetra-bonded H-bond network of water. A fitting procedure indicates that the frequency of this band increases with addition of sugar, and the increase is more marked for trehalose (table 1). This frequency increase reflects the strengthening of intermolecular O–H interactions in the H-bond network of bulk water with addition of sugar. This strengthening suggests a less flexible tertiary structure of the protein in the presence of sugars.

In the denatured state (373 K), the lineshape of Raman susceptibilities of hydrated lysozyme and ternary mixtures (W_hLT40 plotted in figure 2(b)) are very similar. However, addition of sugar can be characterized by the observation of an additional susceptibility around

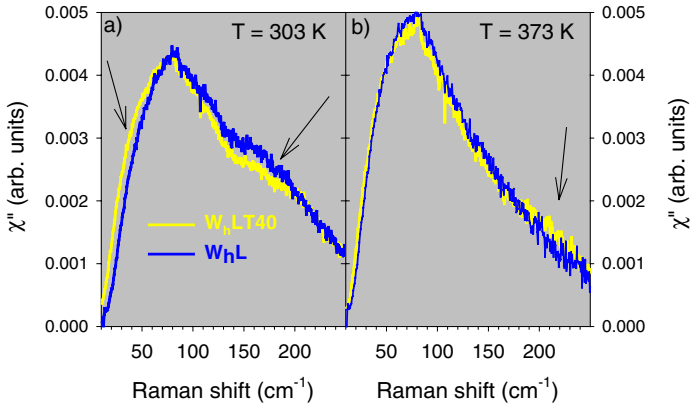

Figure 2. Comparison of Raman susceptibility of hydrated lysozyme (W_hL) and lysozyme dissolved in water–trehalose (W_hLT40) in the native and denatured states.

Table 1. Frequency of the low-frequency band corresponding to the intermolecular O–H stretching vibrations in bulk water, lysozyme–water and lysozyme–water–sugar mixtures.

Samples	Frequency (cm^{-1})
W_hL	191.0 ± 1.2
W_hLM40	194.5 ± 1.3
W_hLS40	193.0 ± 1.5
W_hLT40	198.5 ± 0.7

200 cm^{-1} (localized by the arrow in figure 2(b)). Consequently addition of sugar seems to stabilize the distorted H-bond network of bulk water, and thus the native tertiary structure of the protein.

3.2. In the amide I band region

The Raman spectrum of hydrated lysozyme and the three ternary mixtures (W_hLM40, W_hLS40 and W_hLT40) in the 1500–1765 cm^{-1} spectral range is dominated by a broad Raman band near 1657 cm^{-1} corresponding to the C=O stretching vibration (amide I band) of amide groups coupled to the in-phase bending of the N–H bond and the stretching of the C–N bond [22]. An extreme similarity between the Raman spectra of the amide I band is observed, in accordance with previous studies [23, 24], indicative of a similar secondary structure in a sugar or water environment.

The analysis of this band during heating allows us to monitor the transformation of the molecular conformation, i.e. the unfolding of the α-helix secondary structure.

The temperature dependence of the amide band frequency is fitted by

$$\nu = [(\nu_N - \nu_D)/(1 + \exp((T - T_m)/\Delta T))] + \nu_D,$$

where T_m is the transition midpoint temperature, $2 \times \Delta T$ corresponds to the temperature domain of the transition, and ν_N, ν_D are the frequencies of the amide band in the native and denatured states. A least squares fit of experimental data is plotted in figure 3(a) for the ternary mixtures and for hydrated lysozyme. T_m and ΔT are reported in table 2. It is clearly observed that addition of sugars leads to a shift of the unfolding curve toward high temperature, the most important shift corresponding, as expected, to trehalose. It is also noticeable that the unfolding

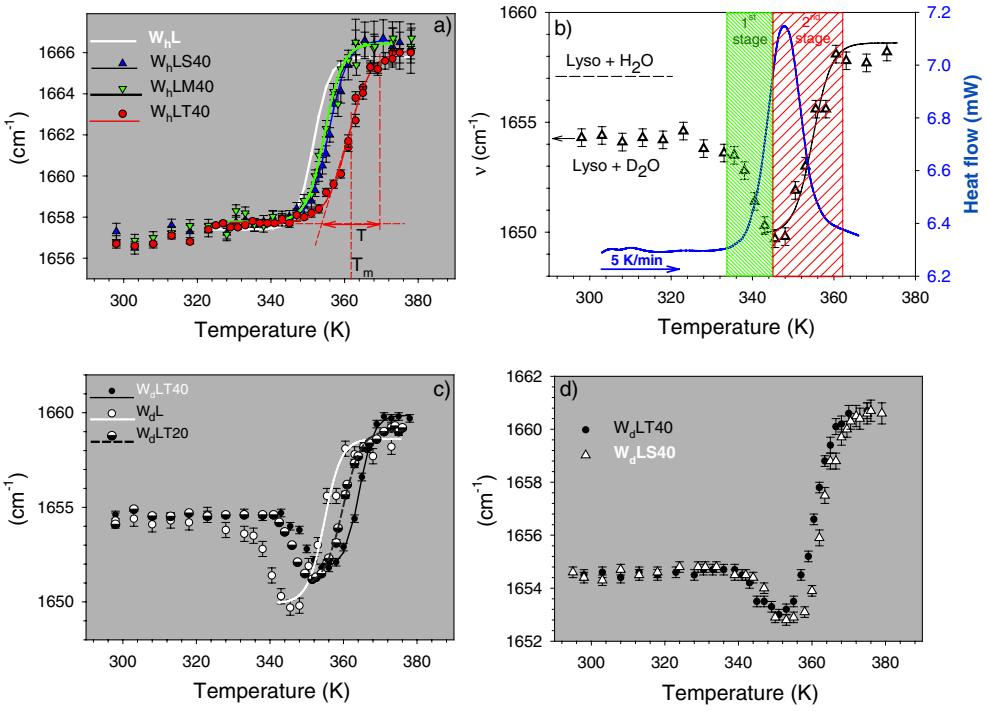

Figure 3. Temperature dependence of the amide I band frequency. (a) For hydrated lysozyme, and lysozyme–water–sugar ternary mixtures. T_m and ΔT reported in table 2 are represented for the W_hLT40 mixture. For hydrated lysozyme, only the fitting curve is reported for clarity. (b) For lysozyme dissolved in D_2O. Crossed zones indicate the two stages of thermal denaturation; the transformation of the tertiary structure accompanied by solvent penetration (first stage), and the unfolding process (second stage). The plot of the denaturation endotherm (obtained from [16]) can be used to determine approximately each contribution to the enthalpy of denaturation. The dashed line represents the frequency of the amide I band in lysozyme dissolved in H_2O. (c) For lysozyme dissolved in D_2O (W_dL), in D_2O + trehalose 20% (W_dLT20), and in D_2O + trehalose 40% (W_dLT40). (d) For lysozyme dissolved in D_2O + sucrose 40% (W_dLS40) and in D_2O + trehalose 40% (W_dLT40). Symbols correspond to experimental data and lines to the fitting procedure using the function given in the text.

Table 2. Parameters of the unfolding process in lysozyme obtained from the analysis of the amide I band.

Samples	T_m (K)	ΔT (K)
W_hL	351.6 ± 0.3	2.2 ± 0.2
W_hLM40	354.5 ± 0.3	2.7 ± 0.2
W_hLS40	355.8 ± 0.3	2.6 ± 0.2
W_hLT40	361 ± 0.3	3.1 ± 0.2
W_dL	354.1 ± 0.3	2.3 ± 0.2
W_dLT20	360.1 ± 0.3	2.6 ± 0.2
W_dLT40	364.3 ± 0.3	2.5 ± 0.2

process is observed for hydrated lysozyme at a temperature slightly higher than 345 K. At this temperature the low-frequency spectrum shows that the H-bond network of water is broken.

A more detailed inspection of figure 3(a) and table 2 reveals that the unfolding process spread over a larger temperature range in ternary mixtures than in hydrated lysozyme, and ΔT

increases, especially in the W_hLT40 sample. Consequently, addition of sugars leads to the extension of the temperature range over which the unfolding process of the secondary structure is observed.

The temperature dependence of the frequency of the amide I band is reported in figure 3(b) for lysozyme dissolved in D_2O(W_dL) to be compared with the heat-flow trace obtained from a previous study [16]. The frequency of the amide I band at room temperature is lowered with respect to the W_hL sample. This frequency lowering was interpreted as a consequence of the NH/ND exchange. Figure 3(b) clearly reveals an additional lowering observed by heating. This latter was associated with solvent penetration inside the protein which is only possible in a highly flexible tertiary structure. The low-frequency analysis indicates that the higher flexibility of the protein is probably induced by the breaking of the H-bond network of water, which exerts a compressive stress on the protein. The unfolding process is observed after solvent penetration, probably because the subtle balance between hydrophobic and hydrophilic interactions is broken. Figure 3(b) clearly shows the two different stages of the thermal denaturation, corresponding to two different contributions to the denaturation endotherm, not identifiable by differential scanning calorimetry.

The analysis of the amide I band for W_dLT40, W_dLT20 ternary mixtures, and lysosyme + D_2O (W_dL) is reported in figure 3(c). The frequency of the amide I band in the folding state is nearly the same in all three samples. This is indicative that water–protein interactions in the native state of lysozyme are similar in all samples with D_2O. The downshift of the amide band frequency is observed at a temperature dependent on the sugar content. This can be understood from the consideration that addition of sugar stabilizes the native tertiary structure. The magnitude of the frequency downshift, i.e. the H/D exchange in the protein interior, is also observed to be dependent on sugar concentration in mixtures, reflecting that water–protein interactions in the interior of the protein are controlled by sugars in the first stage of the thermal denaturation. It was shown that addition of sugar induces a high stability of the distorted H-bond network of water on heating, leading to a relatively compact transient tertiary structure of the protein, which could have lesser hydrophobic surface in contact with the solvent. In this context, figure 3(c) reveals that addition of sugar extends the stability domain of the native tertiary structure and induces a reduction of hydrophobic groups in contact with solvent, which can also be inherent to a reduction of the solvent accessibility in the protein interior.

The unfolding curve was also analysed for W_dLS40 and W_dLT40 ternary mixtures and plotted in figure 3(d). Surprisingly, it is clearly observed that trehalose dissolved in D_2O is not the best stabilizer of the secondary structure of the protein. This confirms that water–sugar interactions are crucial in the sugar bioprotective mechanism.

4. Discussion

This paper clearly shows disaccharide-induced thermostabilization of the lysozyme structure at high temperatures, and more particularly the most bioprotective effectiveness of trehalose (dissolved in H_2O) to preserve folding helical molecular conformation upon heating. The mechanisms by which sugars stabilize proteins were analysed from the study of the influence of sugars on the two-stage process of lysozyme thermal denaturation described in figure 3(b).

Table 1 shows that addition of sugar leads to the distortion of the H-bond network of water, characterized by stronger O–H interactions in the presence of sugars. The strengthened H-bond network of bulk water surrounding the protein induces less flexibility of the tertiary structure in the presence of sugars. The main consequence is the stabilization of the native tertiary structure on an extended temperature range (directly observed in figure 3(c)), and then shifts the first stage of thermal denaturation toward high temperatures. Addition of trehalose leads

to the most increased extension of the stability domain of the native tertiary structure. Sugars also contribute to preserve the very subtle equilibrium between hydrophobic and hydrophilic interactions responsible for the stability of the folding helical conformation, since most of the nonpolar groups are buried out of contact with water in the interior of the protein in its native state. This consideration can be confirmed by the limitation in the downshift of the amide I band frequency, by addition of sugar (figure 3(c)) prior to the unfolding process of the secondary structure in W_dLT samples.

The influence of sugars on the second stage of denaturation (the unfolding process of the secondary structure) corresponding to an increase of ΔT with addition of sugar (table 2, figure 3(a)), can be explained from the consideration that a lower exposure of hydrophobic surface to the solvent, induced by a more compact tertiary structure, extends the unfolding process. Figure 3(d) highlights that water–sugar interactions also have a significant influence on the unfolding process, since the unfolding curves are quite different for lysozyme dissolved in W_dT40 and W_dS40 mixtures, while the first stage of denaturation is very similar in both cases.

It is well accepted that trehalose has privileged interactions with water that are considered as responsible for the strong destructuring effect on the H-bond network of water [10–13]. This property is probably at the origin of the strongest intermolecular O–H interactions in the H-bond network of water leading to the stabilization of the native tertiary structure. The present study carried out on ternary mixtures with high water content undeniably demonstrates that this specific influence of trehalose on the structure of the H-bond network of water is at the origin of the exceptional capabilities to preserve biological functions of lysozyme on heating. Moreover, the analysis of the unfolding process in W_dLT40 and W_dLS40 samples (figure 3(d)) confirms that the characteristics of water–sugar interactions are involved to a great extent in the sugar-induced thermostabilization mechanism. It was found, from molecular dynamics simulation (MD) in agreement with Raman scattering experiments [25], that the H-bond network of water is more perturbed by the presence of trehalose than with sucrose or maltose. This result is explained by the higher hydration number determined by MD [25] in trehalose/water solutions, i.e. by the higher ability of trehalose to form H-bonds with water. Taking into account the common properties of trehalose, sucrose and maltose sugars related to the same chemical formula, it appears that the molecular conformation of trehalose is a preponderant parameter involved in the mechanism of sugar bioprotection. The enhanced hydrophobic character of trehalose with regard to other sugars is also probably at the origin of its ability to stabilize the secondary structure inside the transformed tertiary structure, if it is considered that the solvent penetration inside the tertiary structure breaks the equilibrium between hydrophobic and hydrophilic interactions. However, it is worth noting that the greatest bioprotective effectiveness of trehalose on heating with regard to sucrose and maltose results from the very noticeable and cumulative superiority of trehalose to preserve both the native state of the tertiary structure (the first stage of denaturation) and the unfolding state of the secondary structure inside the transformed tertiary structure (the second stage of denaturation).

References

[1] Sola-Penna M and Meyer-Fernandes J-R 1998 *Arch. Biochem. Biophys.* **360** 10–4
[2] Kreilgaard L *et al* 1998 *Arch. Biochem. Biophys.* **360** 121–34
[3] Xie G and Timasheff S N 1997 *Biophys. Chem.* **64** 25–43
[4] Crowe J H, Leslie S B and Crowe L M 1994 *Cryobiology* **31** 355–66
[5] Green J L and Angell C A 1989 *J. Phys. Chem.* **93** 2880–2
[6] Branca C *et al* 1999 *J. Chem. Phys.* **111** 281–7
[7] Branca C *et al* 2001 *Phys. Rev.* B **64** 224204

[8] Branca C *et al* 1999 *J. Phys.: Condens. Matter* **11** 3823–32
[9] Magazu S *et al* 2004 *Biophys. J.* **86** 3241–9
[10] Branca C *et al* 2002 *Physica* A **304** 314–8
[11] Branca C *et al* 2005 *J. Chem. Phys.* **122** 174513
[12] Lerbret A *et al* 2005 *Carbohydr. Res.* **340** 881–7
[13] Lerbret A *et al* 2005 *J. Phys. Chem.* B **109** 11046–57
[14] Kaushik J K and Bhat R 2003 *J. Biol. Chem.* **278** 26458–65
[15] Caliskan G *et al* 2003 *J. Chem. Phys.* **118** 4230–6
[16] Hédoux A *et al* 2006 *J. Chem. Phys.* **124** 14703–9
[17] Novikov V N *et al* 1995 *J. Chem. Phys.* **102** 4691–8
[18] Saviot L *et al* 1999 *Phys. Rev.* B **60** 18–21
[19] Hedoux A *et al* 2001 *Phys. Rev.* B **63** 144202
[20] Paciaroni A, Bizzarri A R and Cannistraro S 1999 *Phys. Rev.* E **60** R2476–9
[21] Diehl M *et al* 1997 *Biophys. J.* **73** 2726–32
[22] Surewicz W K, Mantsch H H and Chapman D 1993 *Biochemistry* **32** 389–94
[23] Caliskan G *et al* 2004 *J. Chem. Phys.* **121** 1978–83
[24] Leslie S B *et al* 1995 *Appl. Environ. Microbiol. J.* **61** 3592
[25] Ionov R *et al* 2006 *J. Non-Cryst. Solids* **352** 4430–6